

Temporal preconditioners for marching-on-in-time-based time domain integral equation solvers

Hüseyin Arda ÜLKÜ*

Department of Electronics Engineering, Faculty of Engineering, Gebze Technical University, Kocaeli, Turkey

Received: 15.06.2016

Accepted/Published Online: 11.11.2016

Final Version: 30.07.2017

Abstract: Temporal preconditioners to stabilize the marching-on-in-time (MOT)-based time domain integral equation (TDIE) solvers are proposed. Exponentially decaying functions are used as temporal preconditioners and the proposed scheme is applied to analyze scattering from perfect electrically conducting objects using the second-order formulation. The effectiveness of the proposed scheme is demonstrated via numerical examples. It is shown that the temporal preconditioners stabilize the MOT system and the solution. In addition, the initial condition problem of TDIEs is investigated by extending the second-order formulation of the time domain electric field integral equation to the time domain magnetic and combined field integral equations.

Key words: Marching-on-in-time method, time domain integral equations, stability, time domain analysis, transient analysis

1. Introduction

Marching-on-in-time (MOT)-based time domain integral equation (TDIE) solvers are plagued with stability problems. In the literature, many methods have been developed to enhance the stability of MOT-based solvers. These methods are mainly based on semianalytical calculation of MOT matrix elements [1–4], development of specially tailored temporal basis functions [5,6], use of high-order temporal Galerkin testing [7,8], and time domain Calderon projector-based preconditioners [8–10]. Some of these methods increase the computational cost because either they were initially developed in the frequency domain and then extended to the time domain or they require high-order discretization.

One of the problems of the MOT-based solvers is the initial condition problem, i.e. the solution might have linearly increasing or constant components. This problem is not related to low-frequency breakdown [5,11] or inner resonance [12] problems, and it is speculated that these components are caused by improper imposition of the initial conditions [13] or static loops formed in the geometrical mesh [14]. To remedy this problem, a method was proposed in [13] that uses an intermediate variable to formulate and solve the temporal integration of the time domain electric field integral equation (TD-EFIE) for perfect electrically conducting (PEC) scatterers. As a result, the current density function, which is the unknown of interest, is free of linearly increasing or constant components, whereas the intermediate variable, which is the direct solution of discretized MOT matrix system, still contains them. Therefore, these components can corrupt the intermediate variable, especially when a large number of time steps is required.

*Correspondence: hauku@gtu.edu.tr

In this paper, second-order formulation of the TD-EFIE [13] is extended to time domain magnetic and combined field integral equations (TD-MFIE and TD-CFIE) and the concept of temporal preconditioning of MOT-based TDIE solvers is introduced to obtain a nonincreasing and vanishing solution for the intermediate variable. Exponentially decaying functions are used as right and left temporal preconditioners for the MOT matrix system. The proposed temporal preconditioning scheme is applied to the MOT solution of the second-order formulation of the TD-MFIE, TD-EFIE, and TD-CFIE for PEC scatterers. Because of exponentially decaying functions, the solution, i.e. the intermediate variable, vanishes with time, as well as the stability of the MOT matrix system are guaranteed. The proposed preconditioning scheme can be applied directly in the time marching stage without modifying the MOT matrices, and the speed of decay can be controlled by a parameter known as the relaxation coefficient. The effectiveness of the temporal preconditioning is demonstrated via numerical examples. In addition, the effect of the initial value on the MOT solution is investigated and it is shown that the order of the temporal derivative in the integral equation causes linearly increasing and constant contributions.

The rest of the paper is organized as follows: in Section 2.1, the MOT formulation of temporal integration of the TD-CFIE using an intermediate variable is shown. In Section 2.2, temporal preconditioning of the MOT system using exponentially decaying functions is formulated. In Section 3 numerical examples are presented, and in Section 4 conclusions are drawn.

2. Formulation

2.1. Marching on in time

The TD-CFIE for PEC scatterers residing in a linear, nonmagnetic, lossless, and nondispersive homogeneous background medium is traditionally given in terms of current density $\mathbf{J}(\mathbf{r}, t)$, and the derivative of the equation is discretized and solved using the MOT method to find the unknown $\mathbf{J}(\mathbf{r}, t)$ [12]. The temporal derivative cancels the temporal integration in the scalar potential and hence all MOT matrix elements have finite interaction duration depending on the size of the spatial basis function and duration of the temporal basis function. On the other hand, in the method presented in [13], temporal integration of the TD-EFIE is discretized and an intermediate variable $\mathbf{P}(\mathbf{r}, t)$ is defined to cancel out the temporal integrations in the TD-EFIE as $\mathbf{J}(\mathbf{r}, t) = \partial_t^2 \mathbf{P}(\mathbf{r}, t)$, where ∂_t denotes the temporal derivative. $\mathbf{J}(\mathbf{r}, t)$ and $\mathbf{P}(\mathbf{r}, t)$ are expanded as

$$\mathbf{J}(\mathbf{r}, t) = \sum_{n=1}^N \sum_{i=1}^{N_t} \{\mathbf{J}_i\}_n T_i(t) \mathbf{f}_n(\mathbf{r}), \tag{1}$$

$$\mathbf{P}(\mathbf{r}, t) = \sum_{n=1}^N \sum_{i=1}^{N_t} \{\mathbf{P}_i\}_n T_i(t) \mathbf{f}_n(\mathbf{r}), \tag{2}$$

where \mathbf{J}_i and \mathbf{P}_i are unknown coefficient vectors at the i th time step, $T_i(t) = T(t - i\Delta t)$ is shifted interpolation functions, Δt denotes time step size, and $\mathbf{f}_n(\mathbf{r})$ is the spatial basis function. Substituting Eq. (2) in the temporal integration of TD-CFIE, applying point testing in time at $t = j\Delta t$, and Galerkin testing in space to the resulting equation yield the MOT system in terms of the intermediate variable $\mathbf{P}(\mathbf{r}, t)$:

$$\mathbf{Z}_0 \mathbf{P}_j = \mathbf{V}_j - \sum_{i=\max\{1, j-N_g\}}^{j-1} \mathbf{Z}_{j-i} \mathbf{P}_i, \tag{3}$$

where $N_g = \lfloor D_{\max}/(c_0\Delta t) + N_{temp} \rfloor$ [15], D_{\max} is the maximum distance between observation and source points, N_{temp} is the duration of $T(t)$ in time steps to past ($T(t)$ is assumed to be causal), and c_0 is the speed of light in the surrounding medium. The elements of the tested incident field vector \mathbf{V}_j and the MOT matrices \mathbf{Z}_{j-i} are

$$\begin{aligned} \{\mathbf{V}_j\}_m &= \alpha \langle \mathbf{f}_m(\mathbf{r}), \partial_t^{-1} \mathbf{E}^{inc}(\mathbf{r}, t) \rangle_{t=j\Delta t} \\ &\quad + (1 - \alpha)\eta_0 \langle \mathbf{f}_m(\mathbf{r}), \hat{\mathbf{n}}(\mathbf{r}) \times \partial_t^{-1} \mathbf{H}^{inc}(\mathbf{r}, t) \rangle_{t=j\Delta t}, \end{aligned} \quad (4)$$

$$\begin{aligned} \{\mathbf{Z}_{j-i}\}_m &= \frac{(1-\alpha)\eta_0}{2} \langle \mathbf{f}_m(\mathbf{r}), \partial_t T_i(t) \mathbf{f}_n(\mathbf{r}) \rangle_{t=j\Delta t} \\ &\quad + \alpha \langle \mathbf{f}_m(\mathbf{r}), \mathcal{L}\{T_i \mathbf{f}_n, \mathbf{r}, t\} \rangle_{t=j\Delta t}, \\ &\quad - (1 - \alpha)\eta_0 \langle \mathbf{f}_m(\mathbf{r}), \hat{\mathbf{n}}(\mathbf{r}) \times \mathcal{K}\{T_i \mathbf{f}_n, \mathbf{r}, t\} \rangle_{t=j\Delta t} \end{aligned} \quad (5)$$

where $\langle \mathbf{f}_m(\mathbf{r}), \mathbf{b}(\mathbf{r}, t) \rangle = \int_{S_n} \mathbf{f}_m(\mathbf{r}) \cdot \mathbf{b}(\mathbf{r}, t) d\mathbf{r}$, $\mathbf{E}^{inc}(\mathbf{r}, t)$ and $\mathbf{H}^{inc}(\mathbf{r}, t)$ are the band limited incident electric and magnetic field intensities, α is the combination factor of the TD-CFIE, η_0 is the intrinsic impedance of the surrounding medium, and $\hat{\mathbf{n}}(\mathbf{r})$ is the unit normal vector with respect to observation point \mathbf{r} . ∂_t^{-1} denotes temporal integration. In Eq. (5), the TD-EFIE and TD-MFIE operators, $\mathcal{L}\{\cdot, \cdot, \cdot\}$ and $\mathcal{K}\{\cdot, \cdot, \cdot\}$, are defined as

$$\begin{aligned} \mathcal{L}\{T_i \mathbf{f}_n, \mathbf{r}, t\} &= \int_{S_n} \frac{\mu_0}{4\pi R} \mathbf{f}_n(\mathbf{r}') \partial_t^2 T_i(t') \Big|_{t'=t-R/c_0} d\mathbf{r}' \\ &\quad - \nabla \int_{S_n} \frac{1}{4\pi\epsilon_0 R} [\nabla' \cdot \mathbf{f}_n(\mathbf{r}')] T_i(t - R/c_0) d\mathbf{r}', \end{aligned} \quad (6)$$

$$\mathcal{K}\{T_i \mathbf{f}_n, \mathbf{r}, t\} = \nabla \times \int_{S_n} \left[\frac{T_i(t - R/c_0) \mathbf{f}_n(\mathbf{r}')}{4\pi R} \right] d\mathbf{r}', \quad (7)$$

where $R = |\mathbf{r} - \mathbf{r}'|$ is the distance between source and observation points, and ϵ_0 and μ_0 are the permittivity and permeability of the surrounding medium. Once the MOT system in Eq. (3) is solved for \mathbf{P}_i , $i = 1, \dots, N_t$, unknown coefficients for the current density \mathbf{J}_i can be determined using the numerical derivative, e.g., using central difference:

$$\mathbf{J}_i = [\mathbf{P}_{i+1} - 2\mathbf{P}_i + \mathbf{P}_{i-1}]/\Delta t^2. \quad (8)$$

2.2. Temporal preconditioning

The discretized unknown vector of the intermediate variable \mathbf{P}_i can be scaled with the decaying exponential functions $\tilde{\mathbf{P}}_i = \exp[-\sigma t_i] \mathbf{P}_i = \exp[-\sigma i \Delta t] \mathbf{P}_i$ to enforce the vanishing behavior, where σ is the relaxation coefficient. The exponential decay guarantees the convergence of the solution $\tilde{\mathbf{P}}_i$ to zero even if \mathbf{P}_i is linearly increasing. To compensate the effect of the exponential scaling, MOT matrices should be scaled with $\exp[\sigma t_i]$. This process can be regarded as right preconditioning of the MOT matrix system. To prevent the growth in MOT matrix elements, the resulting equation should be scaled with $\exp[-\sigma t_j] = \exp[-\sigma j \Delta t]$, which can be regarded as left preconditioning. As a result, the temporally preconditioned MOT system is given as

$$\tilde{\mathbf{Z}}_0 \tilde{\mathbf{P}}_j = \tilde{\mathbf{V}}_j - \sum_{i=\max\{1, j-N_g\}}^{j-1} \tilde{\mathbf{Z}}_{j-i} \tilde{\mathbf{P}}_i, \quad (9)$$

where $\tilde{\mathbf{V}}_j = \exp[-\sigma j \Delta t] \mathbf{V}_j$ and $\tilde{\mathbf{Z}}_{j-i} = \exp[-\sigma(j-i)\Delta t] \mathbf{Z}_{j-i}$. Since $j \geq i$, the MOT matrix elements $\tilde{\mathbf{Z}}_{j-i}$ always decay with time and the eigenvalues of the companion matrix of the MOT system [16] move inside towards the unit circle through the center. This guarantees the stability of the MOT system as well as the solution $\tilde{\mathbf{P}}_i$. The relaxation coefficient σ can be chosen considering the electrical size of the problem, numerical precision, and total time step size N_t , e.g., $\sigma \propto c_0/(D_{\max} N_t)$ or $\sigma \propto 1/(\Delta t D_{\max} N_t)$.

There are several ways to implement the temporal preconditioner. First, exponential functions can be multiplied by the matrix elements during the matrix filling stage. This requires $O(N^2)$ additional simple multiplication operations. Second, the MOT matrices can be updated after the matrix filling via multiplying the matrix elements by the exponential functions. This multiplication operation is applied once, and since the MOT matrices are sparse, the computational cost of it is $O(N^2)$. In both cases the computational cost of the temporal preconditioner, i.e. $O(N^2)$, is negligible compared to the computational complexity of the MOT scheme, i.e. $O(N^2 N_t)$. It is also possible to fill a precomputed table for the exponential functions $\exp[-\sigma k \Delta t]$, $k = 0, \dots, N_t$, to reduce the cost of the temporal preconditioning further.

3. Numerical results

This section demonstrates the effectiveness of the temporal preconditioning of the MOT scheme via numerical examples. In all examples Rao–Wilton–Glisson (RWG) [17] functions and third-order Lagrange interpolation functions [18] are used as spatial and temporal basis functions, respectively. Unless it is specified, the electric field component of the incident plane wave is $\mathbf{E}^{inc}(\mathbf{r}, t) = \hat{\mathbf{x}}G(t + \mathbf{r} \cdot \mathbf{z}/c_0)$, where $G(t) = \cos(2\pi f_0[t - t_0]) \exp([t - t_0]^2/2\gamma^2)$ is a modulated Gaussian pulse signature with f_0 modulation frequency, f_{bw} essential bandwidth, $\gamma = 7/(2\pi f_{bw})$ duration, and t_0 delay. The MOT matrix elements are determined via the semianalytical method described in [1–3] and algebraic stability analysis is carried out as described in [16]. In all figures the intermediate variables are normalized with c_0^2 (i.e. $\tilde{\mathbf{P}}_i/c_0^2$).

3.1. TD-MFIE

In this example, a unit sphere discretized with $N = 750$ RWG basis functions is analyzed to investigate the effects of the temporal derivative, the initial condition, and the temporal preconditioner proposed in Section 2 on the MOT-TD-MFIE systems. Combination factor $\alpha = 0$, the incident field has $f_0 = 70$ MHz, $f_{bw} = 30$ MHz, and unless otherwise specified $t_0 = 3.5\gamma$. Time step size $\Delta t = 1$ ns.

In Figure 1, one of the current density coefficients obtained by the MOT solution of the TD-MFIE (MFIE), derivative of the TD-MFIE (∂_t MFIE), derivative of the TD-MFIE with delay $t_0 = 3.5\gamma + 50\Delta t$ in incident field (∂_t MFIE_{delayed}), and temporally preconditioned-temporal integration of the TD-MFIE (TP- ∂_t^{-1} MFIE) is shown. For TP- ∂_t^{-1} MFIE, relaxation coefficient $\sigma = 0.004\Delta t^{-1}$. Figure 2 shows the eigenvalues of the companion matrices for the associated MOT systems. The observations on the results given in Figures 1 and 2 can be listed as follows: 1) Comparing the ∂_t MFIE and MFIE results in Figure 1 shows that they agree very well for early time but the ∂_t MFIE result has a constant component whereas the MFIE one vanishes with time. This shows the temporal derivative to be the source of the constant component in the result, as discussed in [13]. Figure 2 supports this conclusion, since some of the eigenvalues of the companion matrix of the MOT- ∂_t MFIE system are located at $z = 1$, whereas the MOT-MFIE system does not have any. 2) The ∂_t MFIE and ∂_t MFIE_{delayed} results in Figure 1 show that the constant levels are on same level with the initial value of the solutions, although they solve for the same MOT matrix system (only the delay of the incident

fields is different). For the delayed incident field, the constant level is lower. It can be concluded that the initial value of the solution is directly related to the incident field at the first time step. Therefore, usually the delay of the incident field is chosen to be very large, which results in a very smooth rise and small constant component levels. 3) In Figure 1, the TP- ∂_t^{-1} MFIE result agrees very well with the MFIE and ∂_t MFIE results, and it does not have any constant component, as expected.

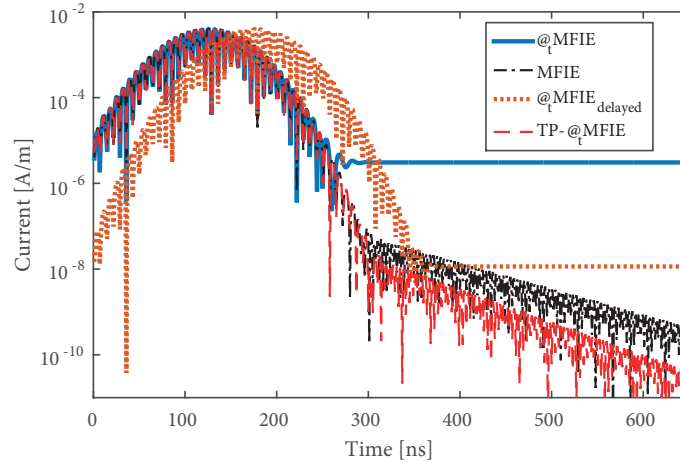


Figure 1. Coefficient of an RWG basis function of the current density for MOT-TD-MFIE systems.

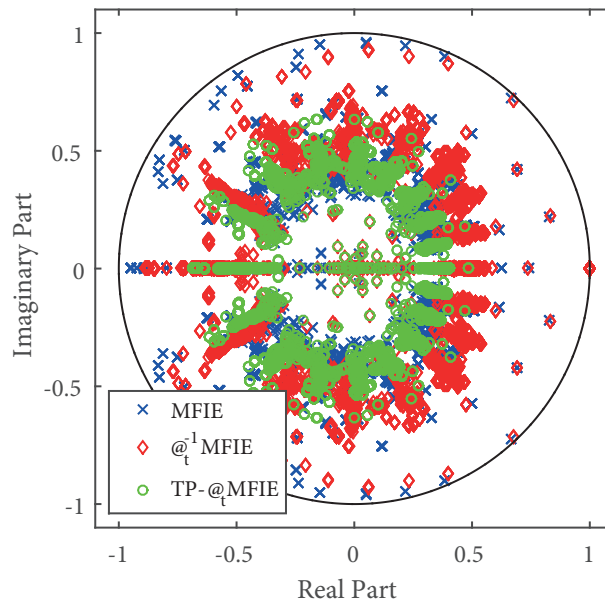


Figure 2. Eigenvalues of the companion matrix of the MOT-TD-MFIE systems.

Figure 3 plots one of the coefficients of the normalized intermediate variables for different relaxation coefficients ($\sigma = \{0, 0.004, 0.01\}\Delta t^{-1}$). In Figure 3 intermediate variable $\tilde{\mathbf{P}}_i$ for $\sigma = 0$ (no temporal preconditioning) still has a constant component but it will be removed on \mathbf{J}_i because of the relation given in Eq. (8). For $\sigma = 0.004\Delta t^{-1}$ and $\sigma = 0.01\Delta t^{-1}$ intermediate variable $\tilde{\mathbf{P}}_i$ also does not have any constant component and results are decaying depending on σ . The eigenvalues of the MOT system for TP- ∂_t^{-1} MFIE ($\sigma = 0.004\Delta t^{-1}$)

in Figure 2, move inside the unit circle and none of the eigenvalues are located at $|z| = 1$. This guarantees the stability of the MOT system and demonstrates the effectiveness of the temporal preconditioning.

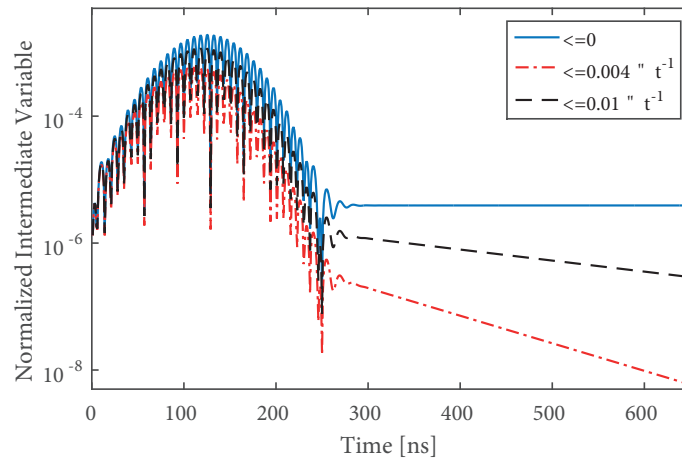


Figure 3. Coefficient of an RWG basis function of the intermediate variable for different relaxation coefficients.

3.2. TD-EFIE

Next the same unit sphere in the previous subsection is analyzed to investigate the effect of temporal preconditioning on the MOT-TD-EFIE system. In this example combination factor $\alpha = 1$, the incident field has $f_0 = 70$ MHz, $f_{bw} = 30$ MHz, $t_0 = 3.5\sigma$, and time step $\Delta t = 1$ ns. For the temporal preconditioner relaxation coefficient, $\sigma = 0.01\Delta t^{-1}$.

Figure 4 plots one of the current density coefficients obtained by the MOT solution of the temporal derivative of TD-EFIE (∂_t EFIE) and the temporally preconditioned-temporal integration of the TD-EFIE (TP- ∂_t^{-1} EFIE), and the coefficient of the associated intermediate variable for TP- ∂_t^{-1} EFIE. In Figure 4, the ∂_t EFIE result has linearly increasing and constant components in the solution due to the improper imposition of the initial conditions [13]. It was also mentioned in [14] that this increasing behavior can be nonlinear due to the iterative solution process. On the other hand, the intermediate variable, as in the solution of the MOT-TP- ∂_t^{-1} EFIE system, has a decreasing behavior, and the current density does not have any linearly increasing or constant components. Figure 5 shows the eigenvalues of the MOT-TP- ∂_t^{-1} EFIE matrix system for different relaxation coefficients. It can be seen that for $\sigma = 0$ (no temporal preconditioning) there are eigenvalues located at $z = 1$, and for $\sigma \neq 0$ these eigenvalues move inside.

This example clearly shows that the proposed method remedies the linearly increasing and constant component problems in the TD-EFIE and improves the stability of the MOT system.

3.3. TD-CFIE-1

In this example a unit sphere discretized with $N = 2430$ RWG basis functions is analyzed to investigate the effect of temporal preconditioning on the MOT-TD-CFIE system. In this example combination factor $\alpha = 0.5$, the incident field has $f_0 = 120$ MHz, $f_{bw} = 40$ MHz, $t_0 = 3.5\sigma$, and time step $\Delta t = 0.625$ ns. For the temporal preconditioner relaxation coefficient, $\sigma = 0.01\Delta t^{-1}$.

Figure 6 plots one of the current density coefficients obtained by the MOT solution of temporal derivative of the TD-MFIE and TD-CFIE (∂_t MFIE and ∂_t CFIE), temporally preconditioned-temporal integration of the

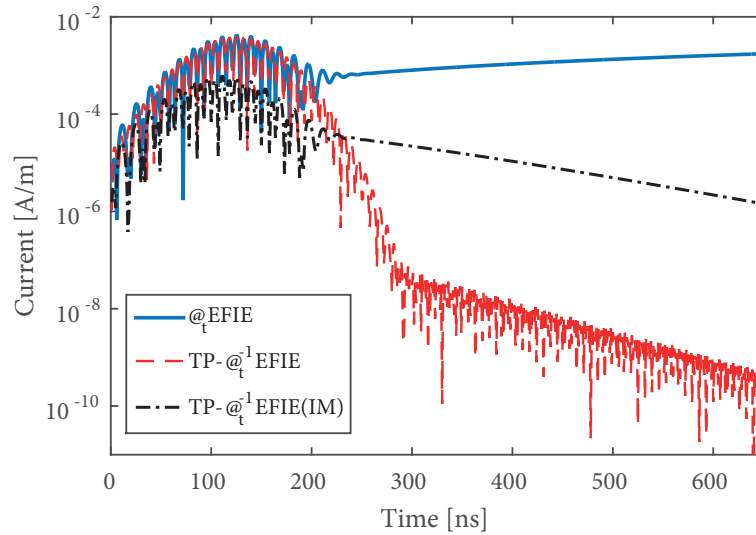


Figure 4. Coefficient of an RWG basis function for MOT-TD-EFIE systems.

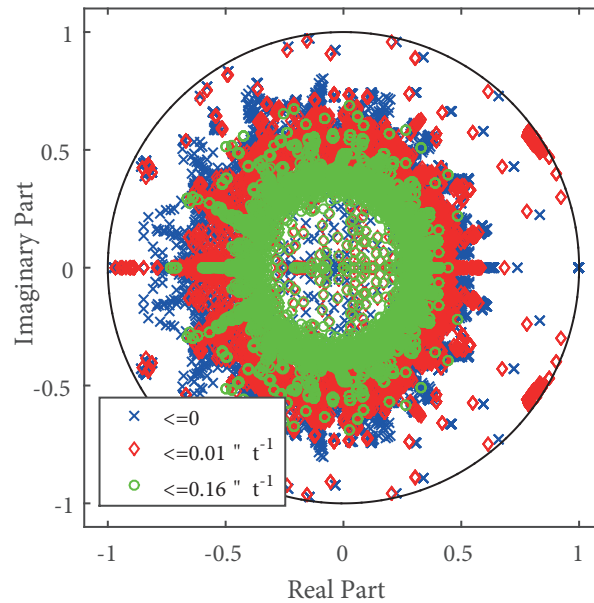


Figure 5. Eigenvalues of the companion matrix of the MOT-TD-EFIE systems for different relaxation coefficients.

TD-CFIE (TP- ∂_t^{-1} CFIE), and coefficient of the associated intermediate variable for TP- ∂_t^{-1} CFIE. It can be seen that the ∂_t MFIE result coincides very well with both CFIE results until 225 ns, but then it has an oscillating behavior due to the inner resonance problem, and the ∂_t CFIE result has a constant component even when it is resonance-free, whereas the TP- ∂_t^{-1} CFIE result does not have any linearly increasing or constant components and vanishes until the numerical accuracy of the MOT scheme. The intermediate variable also decays and vanishes due to temporal preconditioning.

This example shows that the resonance-free TD-CFIE also has a constant component problem, and can be remedied by the proposed method in Section 2.

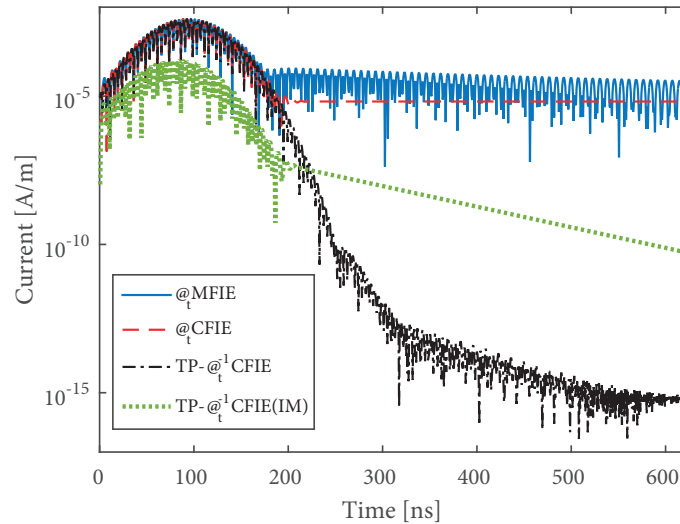


Figure 6. Coefficient of an RWG basis function of the current density for MOT-TD-CFIE and MFIE systems.

3.4. TD-CFIE-2

As the last example, the flower-shaped scatterer described in [6] is analyzed. The scatterer is modeled with $N = 873$ RWG basis functions. In this example combination factor $\alpha = 0.5$ and the electric field component of the incident field is given as

$$\mathbf{E}^{inc}(\mathbf{r}, t) = \hat{\mathbf{x}} \sum_{k=1}^3 G_k(t + \mathbf{r} \cdot \mathbf{z}/c_0), \quad (10)$$

where $G_k(t) = \cos(2\pi f_0[t - t_k]) \exp([t - t_k]^2/2\gamma^2)$ is a modulated Gaussian signature with delay t_k . The incident field has $f_0 = 75$ MHz, $f_{bw} = 25$ MHz, $t_1 = 3.5\gamma$, $t_2 = 3.5\gamma + 250\Delta t$, $t_3 = 3.5\gamma + 500\Delta t$, and time step $\Delta t = 1$ ns. For the temporal preconditioner relaxation coefficient, $\sigma = 0.01\Delta t^{-1}$.

Figure 7 plots one of the current density coefficients obtained by the MOT solution of the temporal derivative of the TD-EFIE and TD-CFIE (∂_t EFIE and ∂_t CFIE), and temporally preconditioned-temporal

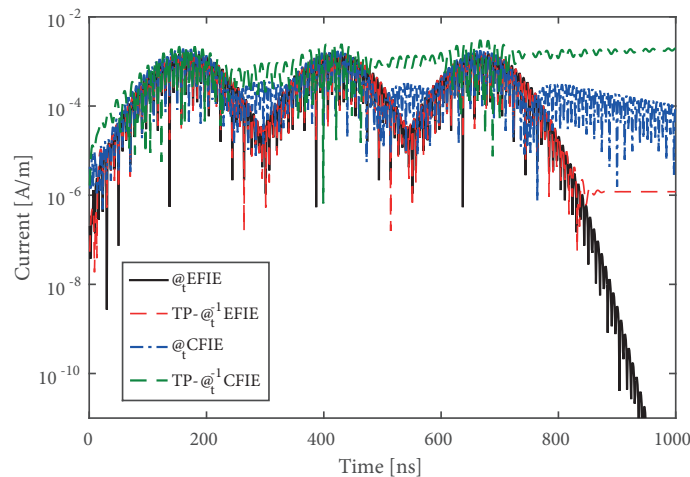


Figure 7. Coefficient of an RWG basis function of the current density induced on the flower-shaped scatterer.

integration of the TD-EFIE and TD-CFIE (TP- ∂_t^{-1} EFIE and TP- ∂_t^{-1} CFIE). As expected, the ∂_t CFIE and TP- ∂_t^{-1} CFIE results coincide very well, except the constant contribution in the ∂_t CFIE result. The TP- ∂_t^{-1} EFIE result coincides reasonably well with CFIE results for main responses; however, for the rest it shows an oscillating behavior due to the inner resonance problem. On the other hand, the ∂_t EFIE result is increasing linearly and does not match the both CFIE results.

This example shows the superiority of the temporal preconditioning and the second-order formulation, especially for the MOT solution of the TD-EFIE.

4. Conclusion

The concept of temporal preconditioning of MOT-based TDIE solvers is introduced and the effectiveness of it is demonstrated by the MOT solution of the TD-MFIE, TD-EFIE, and TD-CFIE for PEC scatterers using the second-order formulation described in [13]. The proposed method does not require any update in the MOT matrix element calculation and can be applied directly to the time-marching part of the MOT solver. It is shown that the temporal preconditioning improves the stability properties of the MOT systems by pushing the eigenvalues of the companion matrix to inside of the unit circle. Note that the temporal preconditioning does not remedy the inner resonance [12] or low-frequency breakdown problems [5,11], and applying it without a postprocessing technique (e.g., filtering or using a second-order formulation) might not be effective.

References

- [1] Ulku HA, Ergin AA. Analytical evaluation of transient magnetic fields due to RWG current bases. *IEEE T Antenn Propag* 2007; 55: 3565-3575.
- [2] Ulku HA, Ergin AA. Application of analytical retarded-time potential expressions to the solution of time domain integral equations. *IEEE T Antenn Propag* 2011; 59: 4123-4131.
- [3] Ulku HA, Ergin AA. On the singularity of the closed-form expression of the magnetic field in time domain. *IEEE T Antenn Propag* 2011; 59: 691-694.
- [4] Shi Y, Xia MY, Chen RS, Michielssen E, Lu M. Stable electric field TDIE solvers via quasi-exact evaluation of MOT matrix elements. *IEEE T Antenn Propag* 2011; 59: 574-585.
- [5] Weile DS, Pisharody G, Chen NW, Shanker S, Michielssen E. A novel scheme for the solution of the time-domain integral equations of electromagnetics. *IEEE T Antenn Propag* 2004; 52: 283-295.
- [6] Wildman RA, Pisharody G, Weile DS, Shanker B, Michielssen E. An accurate scheme for the solution of the time-domain integral equations of electromagnetics using higher order vector bases and bandlimited extrapolation. *IEEE T Antenn Propag* 2004; 52: 2973-2984.
- [7] Beghein Y, Cools K, Bagci H, De Zutter D. A space-time mixed Galerkin marching-on-in-time scheme for the time-domain combined field integral equation. *IEEE T Antenn Propag* 2013; 61: 1228-1238.
- [8] Beghein Y, Cools K, Andriulli F. A DC-stable, well balanced, Calderon preconditioned time domain electric field integral equation. *IEEE T Antenn Propag* 2015; 63: 5650-5660.
- [9] Cools K, Andriulli F, Olyslager F, Michielssen E. Time domain Calderon identities and their application to the integral equation analysis of scattering by PEC objects part I: Preconditioning. *IEEE T Antenn Propag* 2009; 57: 2352-2364.
- [10] Andriulli F, Cools K, Olyslager F, Michielssen E. Time domain Calderon identities and their application to the integral equation analysis of scattering by PEC objects part II: Stability. *IEEE T Antenn Propag* 2009; 57: 2365-2375.

- [11] Chen NW, Aygun K, Michielssen E. Integral-equation-based analysis of transient scattering and radiation from conducting bodies at very low frequencies. *IEE Proc-Microw Anten P* 2001; 148: 381-387.
- [12] Shanker B, Ergin AA, Aygun K, Michielssen E. Analysis of transient electromagnetic scattering from closed surfaces using a combined field integral equation. *IEEE T Antenn Propag* 2000; 48: 1064-1074.
- [13] Ülkü HA, Ergin AA. Solution of the initial condition problem of the time-domain EFIE. In: 2013 Computational Electromagnetics Workshop; 2-5 August 2013; İzmir, Turkey. New York, NY, USA: IEEE. pp. 17-18.
- [14] Shi Y, Bağcı H, Lu M. On the static loop modes in the marching on-in-time solution of the time-domain electric field integral equation. *IEEE Antenn Wirel Pr* 2014; 13: 317-320.
- [15] Yilmaz A, Weile DS, Jin JM, Michielssen E. A hierarchical FFT algorithm (HIL-FFT) for the fast analysis of transient electromagnetic scattering phenomena. *IEEE T Antenn Propag* 2002; 50: 971-982.
- [16] Walker SP, Bluck MJ, Chatzis I. The stability of integral equation time-domain scattering computations for three-dimensional scattering; similarities and differences between electrodynamic and elastodynamic computations. *Int J Numer Model El* 2002; 15: 459-474.
- [17] Rao S, Wilton D, Glisson A. Electromagnetic scattering by surfaces of arbitrary shape. *IEEE T Antenn Propag* 1982; 30: 409-418.
- [18] Aygun K, Shanker B, Ergin AA, Michielssen E. A two level plane wave time-domain algorithm for fast analysis of EMC/EMI problems. *IEEE T Electromagn C* 2002; 44: 152-164.